Platinum and gold nanostructures on silicon via a self-assembled template

Regina Ragan, Sehun Kim, Yong Chen, Xuema Li, R. Stanley Williams
Hewlett-Packard, Quantum Science Research Group, 1501 Page Mill Rd, Palo Alto, Ca USA 94304

ABSTRACT

Parallel arrays of self-assembled rare earth disilicides (erbium and dysprosium) nanowires were grown on Si(001) substrates with nanowire width between 3-10 nm and used as a template for fabricating noble metal (platinum and gold) nanostructure arrays. Submonolayer coverage of platinum and gold were deposited on the nanowire/Si(001) surface post rare earth disilicide growth. Scanning tunneling microscopy and reactive ion etching showed that platinum and gold preferentially deposited on the nanowire surface versus the Si surface. Reactive ion etching of erbium disilicide nanowires with and without platinum on the surface demonstrated that platinum acted as a more resistant etch mask than erbium disilicide. By varying the platinum coverage on the surface we demonstrate the ability to select arrays of nanowire or nanocrystal arrays as a function of platinum coverage.

Keywords: nanowires, nanocrystals, scanning tunneling microscopy, self-assembly.

I. INTRODUCTION

Noble metal nanocrystals (NC) and nanowires (NW) have demonstrated the ability for detection of biological molecules such as DNA and proteins in femtomolar quantities[1] and the strong near field coupling between closely spaced particles leads to a surface enhanced Raman signal that enables single molecule detection.[2] Metal nanocrystals composed of a small number of metal atoms may have chemical reaction selectivity and sensitivity in catalytic processes. Pt nanocrystals are candidates for methanol catalysis where methanol is a hydrogen source for fuel cells. Bulk Pt is poisoned by the carbon monoxide by-product during methanol decomposition; yet Pt nanoclusters are predicted to have catalytic sensitivity. Noble metal NW also have applications in focusing light via surface plasmons and in the propagation of electromagnetic energy in optical circuits. Substantial progress has been made in nanostructure fabrication; however, major challenges still exist in fabricating large-area, high-density, and uniformly-sized ensembles of single crystal metallic NC/NW on substrates.

Hexagonal rare earth disilicide ($RESi_{2-x}$) nanowires self-assemble during epitaxial growth as one-dimensional nanostructures on Si(001) substrates due to an anisotropic lattice mismatch with Si[110].[3] Total energy minimization drives the system to form these one-dimensional nanostructures along Si[110]. The length of coherently strained nanowires is dependent on surface kinetics while the wire width is thermodynamically limited via strain energy.[4] On flat Si(001) substrates, $RESi_{2-x}$ (RE = Dy,[4-6] Er,[4, 7] Gd[4, 8]) nanowires grow in two orthogonal directions due to the double domain 2 × 1 reconstructed Si(001) surface. We have demonstrated that dense arrays of parallel $RESi_{2-x}$ (RE = Er, Dy, Sm) nanowires exhibiting high aspect ratios, having lengths exceeding 1 micron and widths less than 5 nm can be grown on vicinal Si(001) substrates with a miscut of 2.5° toward the [110] azimuth.[9] Vicinal Si(001) substrates with a tilt greater than 2° toward the [110] azimuth exhibit double atomic steps with a single domain 2 × 1 reconstructed surface, that is, Si dimer rows run orthogonal to the step edge.[10] $RESi_{2-x}$ nanowires grow perpendicular to the Si dimer rows and therefore form parallel arrays on vicinal Si(001) substrates. In bulk form and in thin films, $RESi_{2-x}$ are good conductors, $\rho \sim 0.1\ \mu\bullet\Omega$ cm, with a low Schottky barrier to n-type silicon. The highly reactive surface limits applications for $RESi_{2-x}$ nanowires; $RESi_{2-x}$ oxidize rapidly in air. $ReSi_{2-x}$ nanowires can be used as a template for noble metal nanostructure formation.

We have fabricated Pt NC and Pt and Au NW in dense parallel arrays without lithography on Si(001) substrates via $RESi_{2-x}$ templates. The key idea in incorporating different materials with Si is to increase device functionality beyond that of Si integrated circuits while allowing for integration of optics with electronics. We have previously demonstrated that dense arrays of parallel rare earth disilicide ($RESi_{2-x}$,RE = Er, Dy, Sm) metallic nanowires exhibiting high aspect

Nanosensing: Materials and Devices, edited by M. Saif Islam, Achyut K. Dutta,
Proceedings of SPIE Vol. 5593 (SPIE, Bellingham, WA, 2004)
0277-786X/04/$15 · doi: 10.1117/12.569439

ratios, having lengths exceeding 1 micron and widths less than 5 nm can be grown on vicinal Si(001) substrates with a miscut of 2.5° toward the [110] azimuth. We have also demonstrated preferential deposition of Pt on $RESi_{2-x}$ nanowire versus Si(001) surface and that Pt renders highly reactive $RESi_{2-x}$ nanowires air stable. Here, we demonstrate the ability to coat the $RESi_{2-x}$ nanowire surface with another noble metal, Au, and demonstrate the ability to control the type of noble metal nanostructure array via noble metal coverage on the surface and a reactive ion etch (RIE) step. Using self-assembled and unidirectional dense arrays of ($RESi_{2-x}$) as a template, we have fabricated NC (NW) parallel arrays of Pt (Pt and Au) with diameters (width) and interparticle spacings of 3-10 nm over areas greater than 1 square mm. In this paper, we demonstrate that platinum passivates the $ErSi_{2-x}$ nanowire surface. Scanning tunneling microscopy (STM) shows that Pt and Au form clusters on the $RESi_{2-x}$ nanowire surface. Scanning electron microscopy (SEM) images taken after reactive ion etching (RIE) of these nanostructures show that Pt preferentially wets the nanowire surface versus Si and acts as an etch mask. $ErSi_{2-x}$ nanowires without Pt on the surface are significantly etched whereas the Pt coated nanowires are not. Atomic force microscopy images show the nanocrystals arrays have a narrow size distribution.

1. Experiment

$ErSi_{2-x}$ and $DySi_{2-x}$ nanowires were grown on flat and vicinal (2.5 degree miscut from the [110] azimuth) Si(001) substrates in an ultrahigh vacuum (UHV) system. The UHV chamber is also equipped with a scanning tunneling microscope for *in situ* characterization and the base pressure was 1×10^{-10} Torr. The 2 × 1 reconstructed Si(001) surface was prepared by resistively heating the sample to 1150°C for 20 seconds at a chamber pressure of less than 1×10^{-9} Torr, rapidly reducing the temperature to 600° C, and then slowly cooling to room temperature. Er and Dy metal were deposited from an electron beam evaporator on a Si(001) substrate heated to a temperature of 600° C. The Er and Dy coverage was approximately 0.15 ML as determined from *ex situ* Rutherford backscattering (RBS) analysis to calibrate the ion flux with the surface coverage. The pressure during deposition was kept below 1×10^{-9} Torr. $ErSi_{2-x}$ and $DySi_{2-x}$ were formed as a reaction takes place between Si on the surface and the deposited rare earth metal. STM images were taken both before and after rare earth deposition. The sample voltage with respect to the tip during STM imaging was 2.0 V and the images were obtained under a constant tunneling current of 0.1 nA at room temperature. Au was deposited at 550°C on $DySi_{2-x}$/Si(001) surfaces and annealed postgrowth for 30 seconds. Pt was deposited at room temperature on the Si surface after $ErSi_{2-x}$ nanowire formation. The sample was then annealed at 550° C for 10 min. STM images were also obtained after Au and Pt deposition. Samples with $ErSi_{2-x}$ nanowires and Pt/$ErSi_{2-x}$ nanowires were removed from the UHV system and were exposed to ambient briefly and stored in a dry nitrogen environment for a period of approximately one day or less and then etched using RIE in CHF_3 gas for 45 seconds. SEM and atomic force microscopy (AFM) images were obtained before and after etching to view the evolution of the surface structure. AFM was also used to monitor the reactivity of the surface after exposure to air for periods between 5 to 8 weeks.

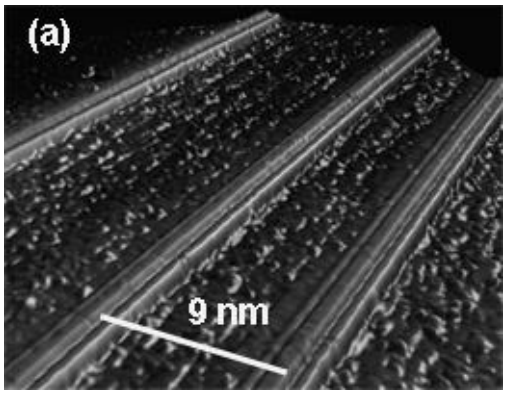

Figure 1: STM image of $DySi_2$ nanowires on Si(001). The nanowires' width is approximately 2 nm.

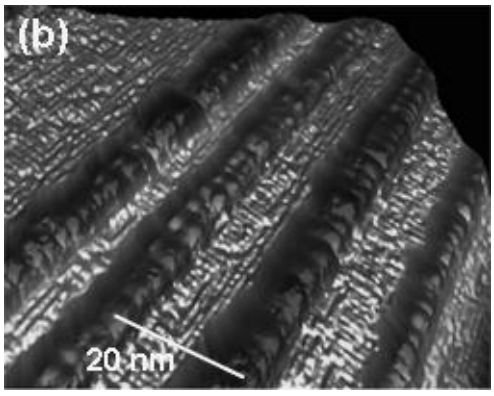

Figure 2: STM image of $DySi_2$ nanowires on Si(001) after Au deposition at 550 °C.

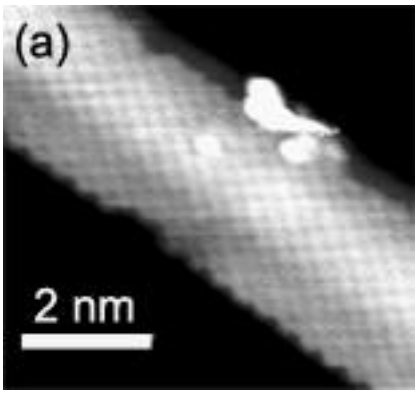

Figure 2(a): 10 nm × 10 nm STM images of $ErSi_{2-x}$ nanowires on Si(001) before Pt deposition the c(2 × 2) surface reconstruction is visible on the nanowire.

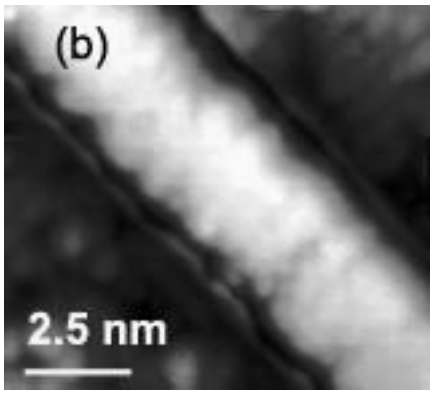

Figure 2(b): After Pt deposition and annealing at 550° C the c(2 × 2) surface reconstruction is gone but the Si (2 × 1) surface reconstruction is still evident in the upper left corner.

2. Results and Discussion

In Fig. 1(a), a typical high resolution STM image of $DySi_{2-x}$ nanowires on Si(001) is shown. The $DySi_{2-x}$ nanowires are composed of bundles of three nanowires. The width of the $DySi_{2-x}$ nanowires in Fig. 1(a) is measured as approximately 2 nm. The STM image shown in Fig. 1(b) is of a $DySi_{2-x}$/Si(001) surface after Au deposition at 550 °C and anneal at the same temperature for 30 seconds. The surface reconstruction has changed. The smooth dy nanowire surface is replaced by a surface that has a periodic surface undulation. This undulation appears to be Au clusters on the nanowire surface. It should also be noted that the 2 × 1 reconstructed Si(001) surface is still visible in the areas not covered by $DySi_{2-x}$ nanowires indicating that Au deposition is preferential on the nanowire surface versus Si. In Fig. 2(a) the $ErSi_{2-x}$ nanowire surface taken *in situ* is shown. The c (2 × 2) surface reconstruction that is characteristic of the hexagonal $ErSi_{2-x}$ lattice is observable. In comparison, an STM image of the nanowire surface after room temperature Pt deposition and post growth annealing at 550° C is shown in Fig. 2(b). The STM image of the Pt coated $ErSi_{2-x}$/Si(001) surface has two significant features. First the c (2 × 2) surface reconstruction is no longer discernible on the nanowire surface. Second, the 2 × 1 surface reconstruction is still evident on the Si surface next to the nanowire. In contrast, sub monolayer coverage of Pt on a bare Si(001) substrate induce disorder of the 2 × 1 surface reconstruction for coverage less than 1/6 ML and induce a c(4 × 2) and c(4 × 6) surface reconstruction for coverage greater than 1/6 ML.[11] The Pt coverage on the surface is 0.1 ML as ascertained from *ex situ* RBS data to calibrate the Er coverage with measured ion current. The coverage of Pt on the nanowire surface appears continuous in this STM image. Therefore, based on the total amount of Pt detected on the surface, it appears that Pt preferentially deposits on the nanowire surface versus the Si(00) substrate.

Further evidence of preferential Pt deposition on the $ErSi_{2-x}$ nanowire surface is obtained from SEM and AFM images taken before and after RIE of the surface. Samples with only $ErSi_{2-x}$ nanowires on the Si(001) surface and samples with Pt deposited on $ErSi_{2-x}$ nanowires on the Si(001) surface were etched in CHF3 gas for 45 seconds. A STM image of $ErSi_{2-x}$ nanowire arrays before etching is seen in Fig. 3(a). The average $ErSi_{2-x}$ nanowire length is approximately 200 nm. After RIE, the SEM image of Fig. 3(b) illustrates that the nanowires are partially etched in CHF_3 gas. The nanowire length has decreased significantly. In comparison, Fig. 3(c) shows the STM image of the Pt/$ErSi_{2-x}$ nanowires arrays on Si(001). Again the average nanowire length is approximately 200 nm. Fig. 3(d) shows an SEM image of Pt/$ErSi_{2-x}$ nanowires after a similar RIE treatment. The majority of Pt/$ErSi_{2-x}$ nanowires remain intact after etching. AFM images were obtained both before and after etching the nanowires to measure the change in nanowire feature height. The average feature height changed from 1.0 nm to 7.8 nm for Pt coated $ErSi_{2-x}$ nanowires and from 1.0 nm to 5.8 nm for the remaining $ErSi_{2-x}$ nanowires with etching.

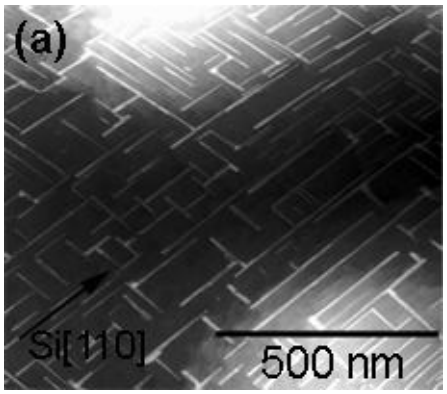

Figure 3(a): STM image of $ErSi_{2-x}$ nanowire arrays on Si(001):

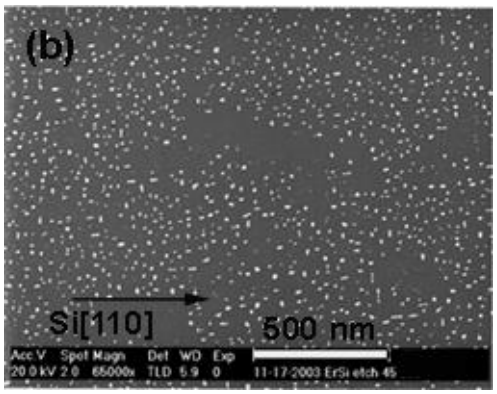

Figure 3(b): SEM image after etching $ErSi_{2-x}$ nanowires in CHF_3 gas.

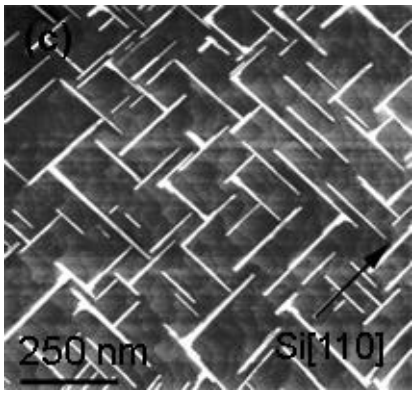

Figure 3(c): STM image of Pt/ $ErSi_{2-x}$ nanowire arrays on Si(001).

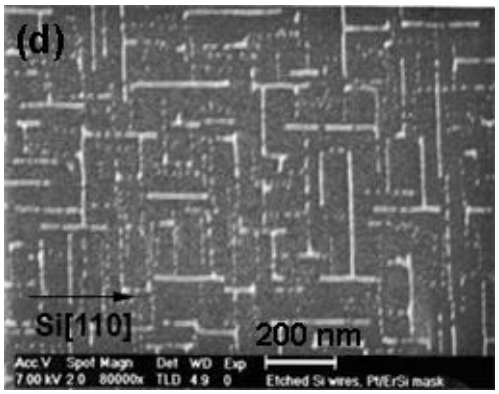

Figure 3(d) SEM image after etching Pt/ $ErSi_{2-x}$ nanowires in CHF_3 gas for 45 seconds.

In Fig. 3(d), some Pt/$ErSi_{2-x}$ nanowires are seen to be segmented after the RIE step. The nanowires that break up into segments or linear chains of quantum dots may arise from incomplete Pt coverage on the surface. STM images prior to etching show clusters on some of the nanowire surfaces. These nanowires may have incomplete Pt coverage. In Fig. 4(a), a 15 nm × 15 nm STM image is shown in which the clusters on the nanowire surface are resolvable. The clusters form an angle of approximately 34.6 ± 4.6 (1σ) degrees with respect to the long axis of the nanowire. The cluster arrangement on the nanowire surface as observed in STM images is consistent with planar clusters of Pt atoms on the surface. This can be understood by comparing the nearest neighbor distance of Pt atoms with that of $ErSi_{2-x}$. The lattice constant of Pt in the face centered cubic (fcc) lattice is 0.3924 nm and that of $ErSi_{2-x}$ in the hexagonal lattice is 0.4088 nm along [0001] and 0.3798 nm along $[11\bar{2}0]$. Due to the anisotropic lattice mismatch with Si $[1\bar{1}0]$, the long axis of the nanowire is oriented along $[11\bar{2}0]$ or the a-axis of the hexagonal lattice.[3] The planes that run at an angle of 38.8 ° with the a-axis of the hexagonal lattice are the $[\bar{1}2\bar{1}3]$ planes and the interplanar spacing of these planes is 0.256 nm. The nearest neighbor spacing of fcc Pt is 0.277 nm but the calculated nearest neighbor spacing for clusters of Pt atoms from density functional theory calculations is 0.258 nm, 0.273 nm, and 0.261-0.265 nm for clusters of 4, 5 and 6 atoms, respectively, and the lowest energy state is in a planar configuration.[12] Thus when the Pt coverage is incomplete on the nanowire surface, it may be energetically favorable for Pt atoms to assemble into a particular cluster size such that the nearest neighbor spacing most closely matches with the $ErSi_{2-x}$ hexagonal lattice. This type of size selection can be exploited in the future to form arrays of metallic quantum dots on Si(001) with a very narrow size distribution. $ErSi_{2-x}$ nanowires that are continuously coated with Pt appear highly strained; AFM images of Pt/$ErSi_{2-x}$ nanowires that were

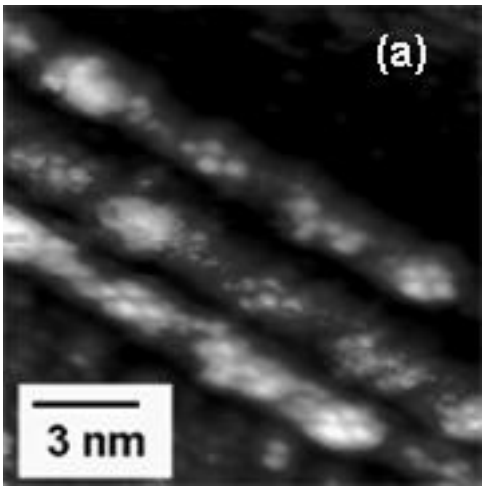

Figure 4(a): 15 nm × 15 nm STM image of Pt clusters on the $ErSi_{2-x}$ nanowire surface after Pt room temperature deposition and anneal at 550° C. The clusters form an angle of 34.6° with the long axis of the nanowire.

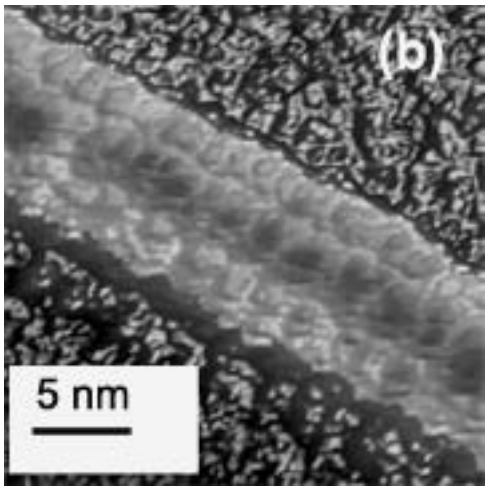

Figure 4(b): 15 nm × 15 nm STM image of Au clusters on $DySi_2$ nanowire surfaces after Au deposition at 550 °C. The Au clusters appear aligned along the long axis of the nanowire.

not etched in the RIE process described above show evidence that the nanowires have delaminated from the surface after sitting in UVH for 7 days. The AFM images have pits on the surface with the approximate width of $Pt/ErSi_{2-x}$ nanowires seen in STM. These pits were not observable in AFM images of surfaces with bare $ErSi_{2-x}$ nanowires or with $Pt/ErSi_{2-x}$nanowires that were treated with RIE within 2 days after preparation. The RIE etch into the Si substrate allows for relaxation of the Si lattice underneath the nanowire and reduce the strain in the $ErSi_{2-x}$ nanowire. Similarly, Au clusters on the $DySi_{2-x}$ surface are visible in the STM image of Fig. 4(b). Yet the Au clusters are aligned along the nanowire's long axis. This can be expected by noting that the lattice parameter along the c-axis of $DySi_{2-x}$, 0.413 nm, has a 1.2% misfit with the lattice constant of Au, 0.408 nm. The lattice mismatch is small enough for coherent epitaxial growth of Au along the c-axis of $DySi_{2-x}$.nanowires.

3. Conclusion

STM images of Pt deposited on $ErSi_{2-x}$ nanowires and Au deposited on $DySi_{2-x}$ fabricated on Si(001) substrates indicate that Pt and Au preferentially deposit on the nanowire surface versus the Si(001) surface. SEM and AFM images confirm that Pt acts as an etch mask for the nanowire surface but not the Si(001) substrate. By varying the Pt coverage on nanowire surfaces either nanocrystals (lower Pt coverage) or nanowires (higher Pt coverage) can be selected. We have also demonstrated that the deposition of Pt on an $ErSi_{2-x}$/Si(001) surface produces air stable metallic nanowires. These self-assembled nanostructures can be used a templates to fabricate hybrid organic-inorganic nanodevices with sensing or computing applications.

ACKNOWLEDGEMENT - The authors wish to acknowledge Ted Kamins and Robert Corn for enlightening discussions and Chengxiang Ji and Doug Ohlberg for help with experiments. We also acknowledge the Department of Advanced Research Projects for supplemental support.

REFERENCE

1. Y. W. C. Cao, R. C. Jin, and C. A. Mirkin, Science **297**, 1536 (2002).
2. M. Moskovits, Reviews of Modern Physics **57**, 783 (1985).
3. Y. Chen, D. A. A. Ohlberg, G. Medeiros-Ribeiro, Y. A. Chang, and R. S. Williams, Appl. Phys. Lett. **76**, 4004 (2000).
4. Y. Chen, D. A. A. Ohlberg, and R. S. Williams, J. Appl. Phys. **91**, 3213 (2002).
5. C. Preinesberger, S. K. Becker, S. Vandré, T. Kalka, and M. Dähne, J. Appl. Phys. **91**, 1695 (2002).
6. J. Nogami, B. Z. Liu, M. V. Katkov, C. Ohbuchi, and N. O. Birge, Phys. Rev. B **63**, 233305 (2001).

7. Y. Chen, D. A. A. Ohlberg, G. Medeiros-Ribeiro, Y. A. Chang, and R. S. Williams, Appl. Phys. A **75**, 353 (2002).
8. D. Lee and S. Kim, Appl. Phys. Lett. **82**, 2619 (2003).
9. R. Ragan, Y. Chen, D. A. A. Ohlberg, G. Medeiros-Ribeiro, and R. S. Williams, J. Cryst. Growth **251**, 657 (2003).
10. D. J. Chadi, Phys. Rev. Lett. **59**, 1691 (1987).
11. H. Itoh, S. Narui, A. Sayama, and T. Ichinokawa, Phys. Rev. B **45**, 11136 (1992).
12. S. H. Yang, D. A. Drabold, J. B. Adams, P. Ordejon, and K. Glassford, Journal of Physics-Condensed Matter **9**, L39 (1997).